A Distributed Model of IPMC

A. Punning*, U. Johanson, M. Anton, M.Kruusmaa, A.Aabloo
Institute of Technology, Tartu University, Nooruse 1, Tartu 50411, Estonia

ABSTRACT

This paper presents a distributed model of an IPMC (Ionomeric Polymer-Metal Composite). Unlike other electromechanical models of an IPMC, the distributed nature of our model permits modelling the non-uniform bending of the material. Instead of modeling solely the tip deflection of the material, we model the changing curvature. Our model of the IPMC describes the actuator or sensor as a distributed one-dimensional RC transmission line. The behavior of the IPMC at its each particular position in time-domain is described by a system of Partial Differential Equations. (PDE). The parameters of the PDE-s have a clear physical interpretation: the conductivity of the electrodes, the pseudocapacitance of the arising double-layer at the boundary of the electrodes, the electric current caused by electrode reactions etc. The electromechanical coupling between the electrical parameters and the bending motion is implemented by means of distribution of electric current along the material in a time domain. The distributed nature of the model permits predicting the non-uniform bending of the IPMC actuators in time domain or to reconcile the output of an IPMC-based position sensor with its shape. Taking into account several nonlinear parameters, the model is consistent with the experimental results even when the inflexion of the actuator or sensor is large or the water electrolysis appears.

Keywords: Ionomeric Polymer-Metal Composite, IPMC actuator, RC transmission lines

1. INTRODUCTION

IPMCs are materials that bend in electric field (Fig. 1). An IPMC actuator consists of a highly swollen polymer sheet, such as Nafion™, filled with water or ionic liquid and plated with metal on both sides. Applied voltage causes the migration of ions inside the polymer matrix which in turn causes the non-uniform distribution of the ions inside the polymer. As a result, the polymer sheet bends. The direction of bending depends on the polarity of the applied voltage. An overview of the working principle of IPMC actuators can be found e.g. in [1].

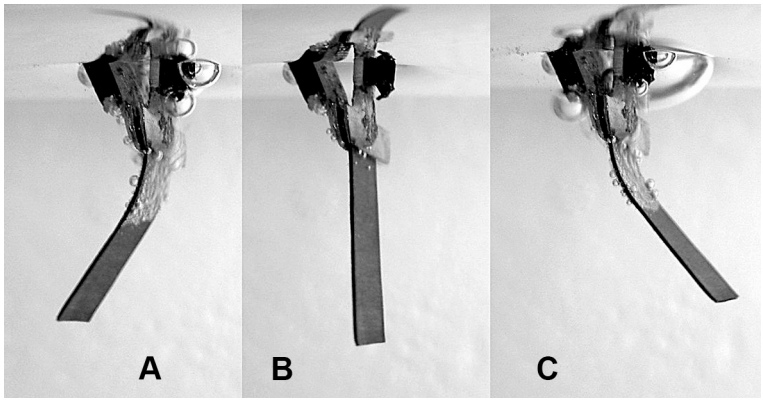

Fig. 1. An IMPC sheet in a bent configuration with the opposite driving voltage polarities (A and C) and an initial configuration with no electric stimulus applied (B).

Several models are proposed so far to model the behavior of IPMC sensors and actuators. A systemized overview of the existing models can be found in [2]. The empirical models describing the behavior of the actuator on a macro-level are derived for example experimentally by curve fitting [3, 4] or based on the description of some sort of an equivalent circuit [5, 6]. To our knowledge, all the equivalent circuit models proposed so far are treated as lumped models. Kanno and Tadokoro have proposed a model in a form of an RC-line but by representing the circuit in a form of a first order

*andres.punning@ut.ee; phone +372 7374832; fax: +372 7374825; http://www.ims.ut.ee

transfer function they reduce it to a lumped model and define the relationship between tensile stress matrix and input current. Also the model proposed by X. Bao et al. [7] is based on the assumption of uniform properties but it is recognized that the distributed model would provide a more accurate description. In [8] a distributed model is proposed, where the IPMC actuator is divided to segments, but each segment is assumed to be driven separately to achieve waving motion of the actuator and each segment is again treated as a lumped model subjected to uniform tensile forces.

The models proposed so far can model the tip displacement or output force of the tip but not the configuration of the entire actuator surface. The model proposed by us is different in the sense that it takes into consideration the fact that deformation of the IPMC material may be non-uniform. Fig, 1 represents a typical behavior of the actuator where the bending curvature from the electric contacts along the sheet decreases.

In this paper we propose modelling the IPMC actuator as a distributed RC transmission line. This presentation permits identifying the electric current through the polymer matrix at every point of the IPMC sheet. As such, it corresponds more accurately to the real situation where the bending curvature of the actuator at each point is determined by the migration of ions at that particular location and variations in the ion concentration. In cantilever configuration the voltage input of the IPMC device is at one location only, but the current from one electrode to the other through the polymer matrix appears over the full device. Due to the nonzero resistance of the metal electrodes a drop of voltage arises along the electrodes, causing the differences of voltage between the opposite sides of the IPMC device. As a result, the voltage perturbation propagates along the device in a wavelike manner. The effect appears noticeably in the case of the IPMCs with lower conductivity of the electrodes (for example made of platinum), but exists in any case as long as there exists the resistance of the electrodes. The non-uniform bending of the IPMC is caused by the non-uniform distribution of voltage between the opposite sides of the IPMC device.

In the current paper we represent the model of an IPMC actuator in an analytical form based on the theory of RC transmission lines and show how to derive the PDEs describing the propagation of voltage for the model. By coupling the current through the polymer matrix to the mechanical bending of the actuator we obtain the electromechanical model of an IPMC. The resulting PDEs are complicated and supposedly difficult to solve, therefore we have made some simplifications to obtain a model valid for some specific IPMC materials only. The step voltage input to this IPMC device is easily solvable in a closed form. We then proceed by representing the simulation results and thereafter demonstrate that these results are well consistent with the experimental data. Finally, we briefly describe a model for a non-linear case that also takes into account the increase of the conductivity of ionomer during electrolysis of solvent.

2. CHARACTERIZATION OF THE ACTUATOR

2.1 Characterization of the shape of the actuator

Generally the models of an IPMC described in the scientific literature do not characterize the shape of IPMC-based devices. These models usually describe the motion of the tip or the blocking force of the tip of the device. The equipment used to characterize the parameters is for instance laser position sensors or force gauges [9, 10].

In order to record and describe the variable shape of the actuator, we developed a simple computer vision system. It consists of a fast CCD camera and a PC with image processing software. The National Instruments Vision was used for both frame grabbing and image processing. The direction of the camera is set transverse to the actuator and the experiment is illuminated from the background through a frosted glass. The image of the actuator recorded in such a way consists of a single curved contrast line. The separate frames of a noticeable bending actuator, recorded in such a way, are depicted in Fig. 2.

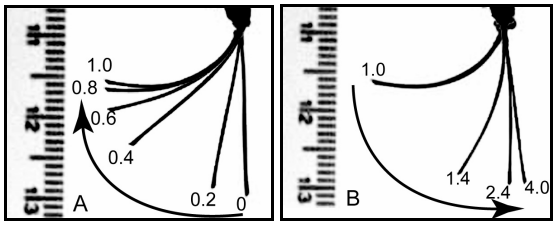

A B

Fig. 2. Overlay of a series of frames showing the response of an actuator to a 1s driving voltage pulse. A – actuation during the pulse; B – relaxation after the pulse. The numeric characters indicate the time instant of the frame.

It is apparent from Fig. 2., that in the beginning of the input pulse (images 0...0.4s in Fig. 2.-A) the actuator performs a sharp motion close to the input contacts only, the free end remains almost straight. Later (images 0.4...1.0s in Fig. 2.-A) the flexure of the actuator propagates gradually on, but the flexure at the region close to the contacts does not increase any more. During the relaxation (images 1.0...4.0s in Fig. 2.-B) the sharp decrease of the flexure takes place close to the input contacts again, whereas the remaining part of the actuator straightens slowly in few seconds.

In order to describe the bending movement of the actuator, the image of the bending sheet is divided into segments assumed to have a constant curvature as depicted in Fig. 4. (angles a1, a2, a3). The angles of the segments are calculated from each frame of the video. The graphs of the angles changing in time describe the possibly nonuniform shape of the sample. A typical changing flexure of the Musclesheet™ actuator is depicted in Fig. 3. It can be observed that the bending of the sheet is faster and stronger close to the input contacts, getting progressively weaker as well as delayed towards the free end of the sheet.

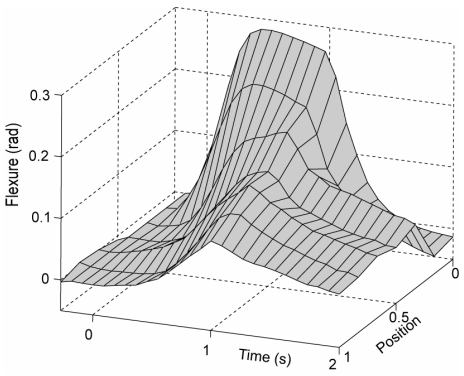

Fig. 3. Mechanical response of an actuator to a step input voltage. The "Position" axis stands for the relative coordinate starting from the input contacts.

2.2 Characterization of the electrical parameters

The drop of voltages along the electrodes of the actuator can be recorded by attaching additional terminals onto its surface. The outline of the setup of the electrical measurements is depicted in Fig. 4.

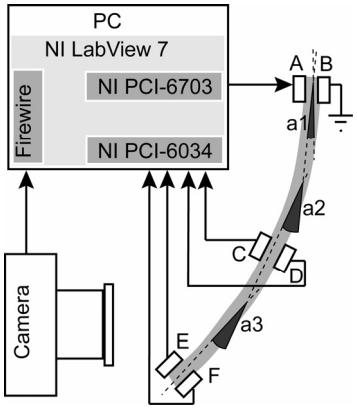

Fig. 4. Setup for our electrical measurements.

We measure the voltages on the surface of a working IPMC-based actuator or sensor by attaching a set of lightweight contact pairs of to its surface using special lightweight clips, and connect them via thin wires to the measuring equipment. The voltages U_C, U_D, U_E and U_F with respect to the ground are measured at the contacts C, D, E and F respectively, as well as the input voltage U_A at the contact A. The voltages between the two faces of the sample can be calculated as $U_C - U_D$, and $U_E - U_F$. The measured voltages on an actuator, bending similarly to the one presented in Fig. 2, are represented as a 3D graph in Fig. 5.

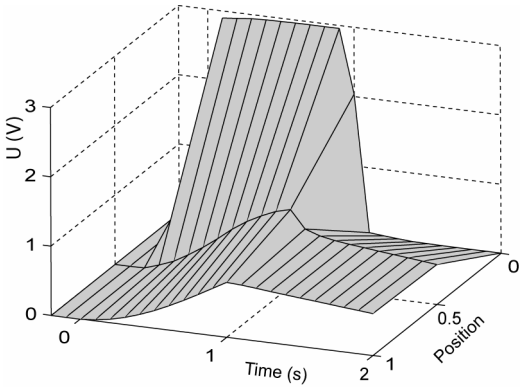

Fig. 5. Voltages along a bending actuator.

3. A DISTRIBUTED MODEL OF IPMC

The fact that the electrical perturbation as well as the change of the flexure spreading along the actuator at finite speed; and the described similarity between the two graphs Fig. 3. and Fig. 5. were the motivations to develop a distributed model of an IPMC.

3.1 The general distributed model of IPMC

The basis of the model is the distributed model of an IPMC proposed by Kanno *et al*. in 1996 [5]. Originally Kanno divided a piece of an IPMC into ten similar segments and modeled the relation between the input current and tip displacement. By dividing the same piece into an infinite number of infinitesimally short similar segments, gives an RC transmission line. Actually, the elaborated model of Kanno models an IPMC as a leaky distributed thin-film capacitor with poor electrode conductivity and considerable shunt losses.

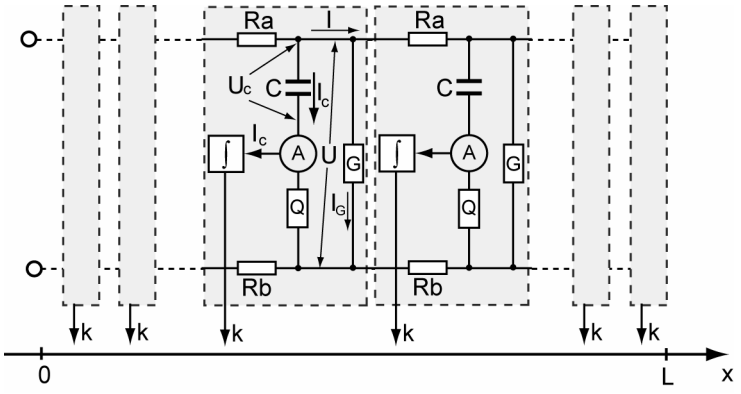

Fig. 6. The distributed model of IPMC.

The distributed model of an IPMC is given in Fig. 6. Besides the capacitor and resistors each single unit of the RC transmission line contains an ammeter measuring current I_C through the capacitance C. Current I_C is integrated with respect to time, resulting to the mechanical response k at the position of the single unit.

The voltage and electric current along the line can be generally represented by Telegrapher's equations [11]. The Telegrapher's equations can be understood as a simplified case of Maxwell's equations. In a more practical approach, one assumes that the line is composed of an infinite series of two-port elementary components, each representing an infinitesimally short segment of the transmission line.

Next we derive the Telegrapher's equations for this model:

The variation of voltage along the line is expressed as:

$$\frac{\partial}{\partial x}u(x,t) = (Ra + Rb)\cdot i(x,t), \tag{1}$$

where $u(x,t)$ is the voltage between the electrodes and $i(x,t)$ is the electric current along the line. From now the parameters Ra, Rb, C, Q and G are per unit length of the sample.

The variation of electric current along the line equals to the sum of currents via the shunting conductance i_G and via the capacitance C i_C:

$$\frac{\partial}{\partial x}i(x,t) = i_G(x,t) + i_C(x,t)\cdot \tag{2}$$

From

$$i_C(x,t) = \frac{u(x,t) - u_C(x,t)}{Q} = C\cdot\frac{\partial}{\partial t}u_C(x,t) \tag{3}$$

the electric current via the capacitance C can be expressed as:

$$i_C(x,t) = \frac{u(x,t)}{Q} - \frac{\int_0^t u(x,t-\tau)\cdot e^{(-\frac{\tau}{Q\cdot C})}d\tau}{Q^2\cdot C} \tag{4}$$

After inserting (4) to (2) we get the second half of the telegrapher's equation:

$$\frac{\partial}{\partial x}i(x,t) = \frac{u(x,t)}{G} + \frac{u(x,t)}{Q} - \frac{\int_0^t u(x,t-\tau)\cdot e^{(-\frac{\tau}{Q\cdot C})}d\tau}{Q^2\cdot C} \tag{5}$$

The equations (1) and (5) form the Telegrapher's equations for the transmission line model of an IPMC. After derivation of (1) with respect to x and using (5) we get the equation for $u(x,t)$:

$$\frac{\partial^2}{\partial x^2}u(x,t) = (Ra + Rb)\left(\left(\frac{1}{G} + \frac{1}{Q}\right)\cdot u(x,t) - \frac{1}{Q^2\cdot C}\cdot\int_0^t u(x,t-\tau)\cdot e^{(-\frac{\tau}{Q\cdot C})}d\tau\right) \tag{6}$$

The mechanical deformation and the electrical parameters of the IPMC can be coupled using the equation from the model of an IPMC proposed by Bao *et al* [7]. In the simplest case the curvature of IPMC at a given point of the sample at a given instant of time depends on the amount of moved electric charges at that point:

$$\frac{\partial}{\partial t}k(x,t) = K\cdot\frac{\partial}{\partial t}q(x,t), \tag{7}$$

where q is an electrical parameter – electric charge of the capacitance C; and k is a geometrical parameter of the actuator – curvature. K is the coefficient for bending effect of the charge moving to the electrode.

The electric charge of capacitance C can be expressed from (8) as (9):

$$u(x,t) = \frac{q(x,t)}{C} + Q\cdot\frac{\partial}{\partial t}q(x,t) \tag{8}$$

$$q(x,t) = \left(\int_0^t \frac{u(x,\tau)\cdot e^{\left(\frac{\tau}{C\cdot Q}\right)}}{Q}d\tau\right)\cdot e^{(-\frac{t}{C\cdot Q})} \tag{9}$$

After solving the equations (6) and (9) for $q(x,t)$ with appropriate boundary conditions and using the equation (7), the curvature of IPMC at a given point of the sample at a given instant of time can be calculated.

3.2 The simplified distributed model

If the value of resistance Q of some casual IPMC material is far lower, than the resistances of the electrodes Ra and Rb, and the value of G is very high, their influence may be neglected as depicted in Fig. 7. In that case the model of IPMC reduces to a lossless transmission line. Using some specific boundary conditions, for example step voltage input, its behavior can be described in a closed form. The step voltage input is easily realizable also in the experiments with the IPMC in order to compare the results with the model. A comprehensive overview of the lossless uniform distributed transmission lines in time domain considering different bounder conditions is presented in [11, 12, 13].

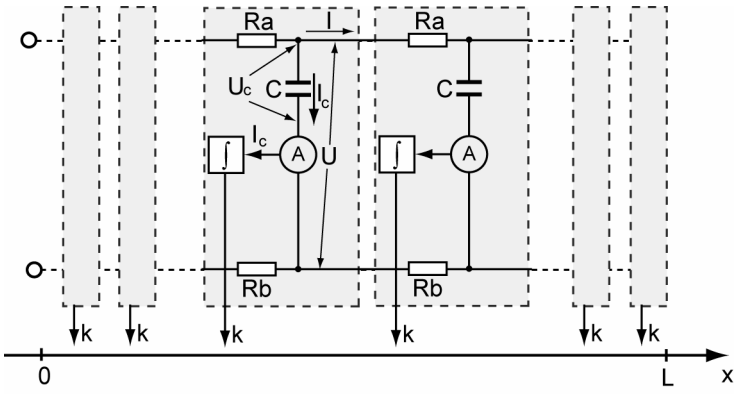

Fig. 7. A simplified model of IPMC, solvable in a closed form.

For the lossless transmission line the equation (6) simplifies to a well-known parabolic PDE – sometimes called a diffusion equation or a heat equation:

$$\frac{\partial^2}{\partial x^2}u(x,t) = (Ra + Rb)\cdot C \cdot \frac{\partial}{\partial t}u(x,t)\cdot \tag{10}$$

An IPMC actuator can be described as an open-ended transmission line having finite length L. The voltage along an open-terminated finite-length uniform RC transmission line under step-voltage excitation is solvable in a closed form and is given by the following formula:

$$U(x,t) = \sum_{n=0}^{\infty}((-1)^n \cdot (erfc((2n+\frac{x}{L})\cdot\sqrt{\frac{(Ra+Rb)\cdot C}{4t}}) + erfc((2n+2-\frac{x}{L})\cdot\sqrt{\frac{(Ra+Rb)\cdot C}{4t}}))) \tag{11}$$

[19,20]. Here Ra, Rb and C are the total resistance and capacitance of the transmission line with the length L, and $erfc(x)$ is the complementary error function.

From the equation (11) the electric current through the capacitance at the position x and time instance t is also solvable in a closed form:

$$I_{dx}(x,t) = \frac{dI(x,t)}{dx} = C\cdot\sum_{n=0}^{\infty}(\frac{(-1)^n}{2t\sqrt{\pi}}\sqrt{\frac{(Ra+Rb)\cdot C}{t}}\cdot(2n+\frac{x}{L})\cdot e^{-\frac{1}{4}(2n+\frac{x}{L})\frac{(Ra+Rb)\cdot C}{t}}\cdot(2n+2-\frac{x}{L})\cdot e^{-\frac{1}{4}(2n+2-\frac{x}{L})\frac{(Ra+Rb)\cdot C}{t}}) \tag{12}$$

The flexure at the given point x at time instance t can be calculated by summarizing all motions generated by all charges before the instant t:

$$k(x,t) = K\cdot\int_0^t I_{dx}(x,t)dt \tag{13}$$

Calculating $I(x,t)$ from (12) and deformation from (13) permits finding the flexure of the actuator at any point x at any time instance t and thus finding the shape of the IPMC actuator for non-uniform bending as a response to a rectangular input voltage pulse.

If the parameters G and Q cannot be neglected, the model behaves as a lossy RC transmission line. The resistance G limits the charging current of the pseudocapacitance C, that in turn diminishes the voltage drop along the electrodes and relieves the non-uniformity of the distribution of the voltage. The conductivity Q diminishes considerably when the electrochemical electrode reactions (for example the electrolysis of the solvent) appear, that in turn increases the voltage drop along the electrodes. Anyway, as long as there exists resistance of the electrodes Ra and Rb, the electric current along the electrodes causes voltage drops and the curvature of the IPMC actuator is not uniform.

4. SIMULATIONS OF THE ELECTROMECHANICAL MODEL

In the following section, we evaluate the model by simulating the voltage distribution, current and curvature of the samples with different parameters. However, it is not possible to measure directly the current through the sheet. This data can be only derived from the simulation. Some simulations of a step response of the actuators with various electrode resistance and capacitance values on similar scales are given in Fig. 8. - Fig. 10. The simulations are performed using equations (11), (12) and (13).

For the Simulation 1. the values of the surface resistances and capacitance are similar to the values measured on a real sample of 30mm long IPMC sheet and are the following: $Ra = 9\Omega$, $Rb = 6\Omega$, $C =$ 100mF. The resistances are measured using a four-probe system and the capacitance is determined from the charging curves.

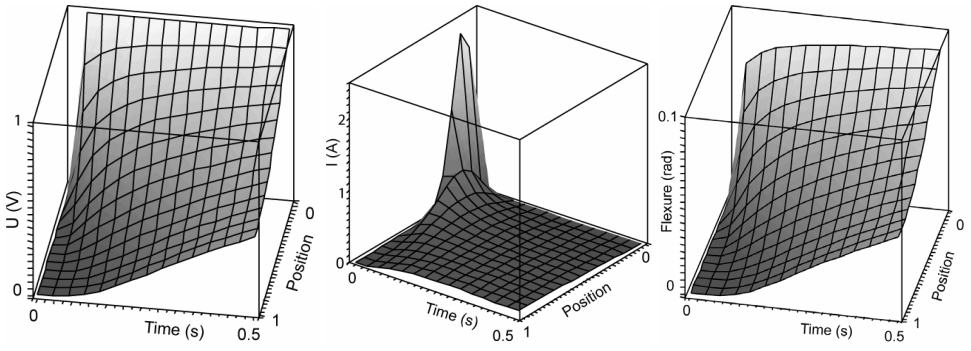

A B C

Fig. 8. Simulation 1. C =0.1F; $Ra + Rb$ =15Ω. A – voltage, B – current, C – flexion.

The 3D graphs demonstrating the voltage and current distribution along the length of the RC transmission line in time space are depicted in Fig.8. On the graphs, the "Position" axis stands for the relative coordinate starting from the input contacts. The graphs demonstrate that voltage increases rapidly close to the input contacts and more slowly further away from the input contacts (Fig. 8.-A). The electric current peaks sharply near the input contacts during the first few milliseconds of the input pulse, and then decreases rapidly to almost zero towards the free end of the sample.

The distribution of current depicted in Fig. 8.-B produces the bending motion of the sample depicted in Fig. 8.-C. The graph exhibits that the actuator performs a sharp movement only close to the input contacts. The noticeably weaker change of the curvature of the free end appears after a short delay. The behavior of the voltage and the flexure are rather similar to the parameters obtained by the measurements of a real actuator and presented in Fig. 5. and Fig. 3. respectively.

Coefficient K of the equation (13) is not determined yet. To obtain the amplitude of the flexure similar to Fig. 3. we applied coefficient K about 3.

There is an obvious similarity between the charts in Fig. 8.-A and Fig. 8.-C. Since current is a derivative of voltage and the curvature, in turn, is the integral of the current, both with respect to time, the similarity is easy to explain.

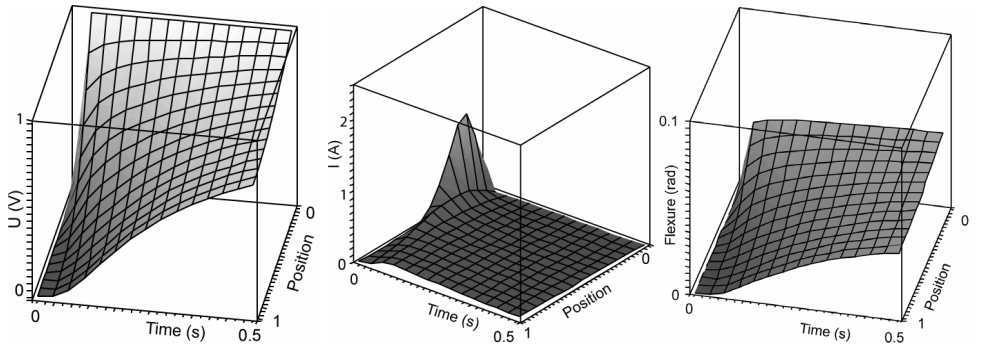

A B C

Fig. 9. Simulation 2. C =0.05F; $Ra + Rb$ =15Ω. A – voltage, B – current, C – flexion.

In Simulation 2 depicted in Fig. 10. the capacitance of the actuator is twice less than in Simulation 1 whereby the resistances of the electrodes remains the same. When compared with the motion of Simulation 1, the motion of Simulation 2 is about twice weaker, whereat the free end gains its maximal position faster. This corresponds to the conclusion of Akle *et al*., that the strain response of an ionomeric transducer is strongly correlated to the capacitance of the plated material. Akle *et al*. demonstrate that there is an approximately linear relationship between strain response per unit voltage and the capacitance of the transducer [14].

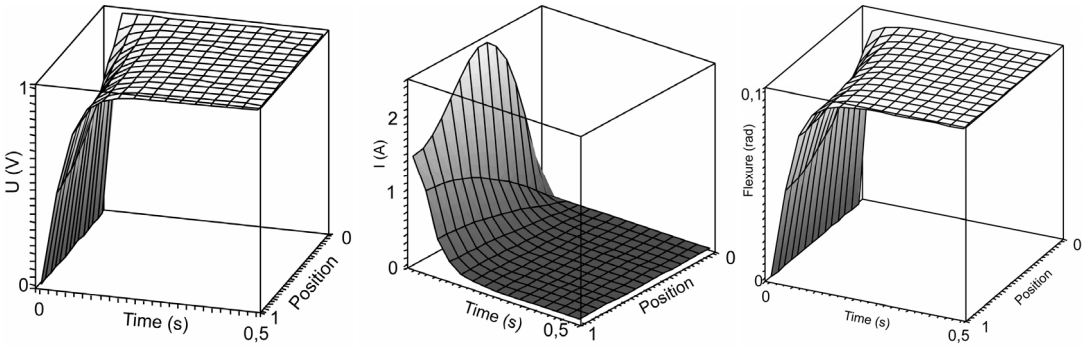

A B C

Fig. 10. Simulation 3. C =0.1F; $Ra + Rb$ =1Ω. A – voltage, B – current, C – flexion.

Simulation 3 depicted in Fig. 11. describes the case, where the resistance of the electrodes is very low whereby the capacitance of the actuator is the same as in Simulation 1. The electric current between the electrodes is high due to the good conductivity of the electrodes, that in turn creates only a subtle voltage drop along the electrodes. The flexure is close to uniform and gains its peak fast. Although the free end of the actuator retards, due to the good conductivity there is no considerable voltage drop along the surface of the actuator and after half of a second already the flexure of the actuator becomes uniform, i.e. forming an arc of a circle. This conclusion is consistent with the observation given in [15] that the lower surface-electrode resistance generates higher actuation capability in the IPMC artificial muscles.

5. IMPLICATIONS AND REFINEMENTS

The presented distributed one-dimensional model of an IPMC consists of a number of lumped models coupling them with a spatial parameter – a generally uneven distribution of voltage caused by the resistance of the electrodes. Its advantages with respect to the previous models are:

- it permits modeling the non-uniform flexure of the IPMC actuator in spatial and time domain.
- it permits modeling large flexure of the actuator or sensor.
- it takes into account the real measurable parameters of the material – resistance of the electrodes and capacitance and with respect to the previously developed models does not reduce it to a uniform lumped model;
- it is scalable, i.e. the length of the actuator is one of the parameters of the model;

- the values of the measurable parameters - the capacitance of the material, the resistance of the electrodes and the length; - may vary on a large scale;
- it contains only one empirical parameter – coefficient K of the equation (7), i.e. the scaling of the flexure;
- a noteworthy exceptional feature of the simplest model described above is the existence of an analytical solution in certain conditions.

The distributed models of IPMC actuators described in chapters 3 and 4 assumed that the driving input voltages are so low, that the electrode reactions, for example the electrolysis of the solvent, do not appear. Measuring the parameters G and Q in the conditions of different voltages between the electrodes gives a well determined relation between the values of the resistors and the voltage applied. A typical behavior of the parameters of Musclesheet™ is presented in Fig. 11. When the amplitude of the voltage approaches the certain level, both resistances decrease fast, finally reaching very low values. The effect can be explained with electrochemical reactions on electrodes, for example the electrolysis of the solvent. In that case the consumption of electric current and electric power through the resistance G is remarkable. The resistance Q limiting the charging current of capacitance practically disappears, and the performance of an actuator is higher. Both parameters have serious influence on the distribution of voltage on the whole device.

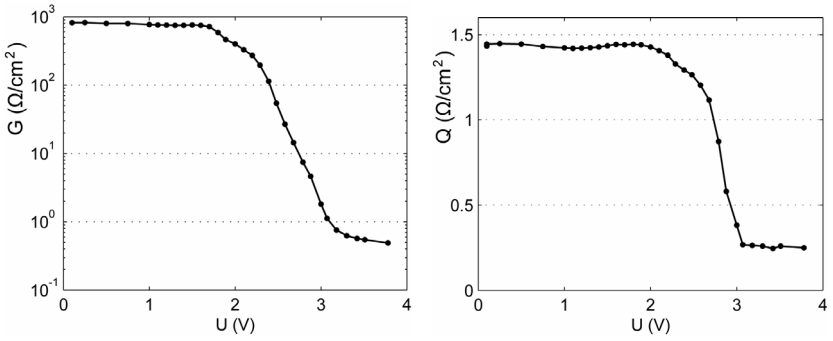

Fig. 11. The typical relation between resistance G and Q and the voltage.

The block diagram of the distributed model of an IPMC considering the electrode reactions is depicted in Fig. 12. The values of the parameters G and Q depend on the actual state of the voltage as $G(x,t) = G_0 \cdot f_1(u(x,t))$ and $Q(x,t) = Q_0 \cdot f_2(u(x,t))$ respectively. The resistor Q limits the charging current of the capacitance C. When the electrode reactions appear, the charging current of the capacitance C grows due to the almost disappearing resistance of resistor Q. That in turn increases the actuation capabilities of the device in that region.

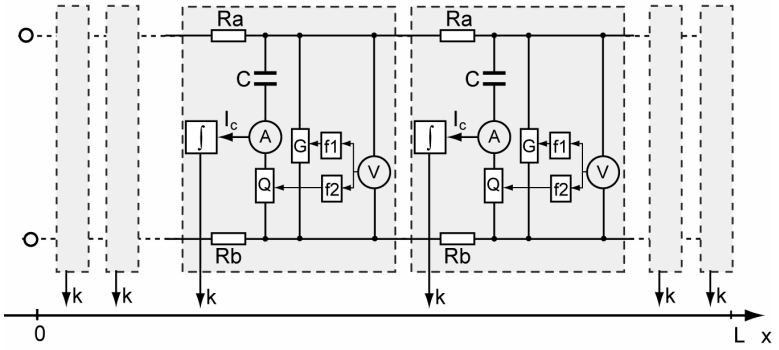

Fig. 12. A model of IPMC considering the electrode reactions.

The models described in the current paper do not take into account the static mechanical parameters of IPMC membranes, for example the viscoelasticity of polymer membranes, the blocking force produced by the IPMC actuator, the mass,, etc. Presumably the combination of the electrical distributed model and the theory of mechanics of beams would give a more accurate result. In order to add the viscoelastic properties of the IPMC materials to the model, the real flexure k_1 should be calculated as a function of the flexure k caused by the relocation of the charged particles inside the IPMC and the viscoelastic parameters of the material (for example elastic modulus E and viscosity n): $k_1(x,t) = f(k(x,t), E, n)$.

6. ACKNOWLEDGEMENTS

This work has been supported by Estonian Ministry of Education, European Science Foundation, Estonian Science Foundation grants No. 6765, 6785 and 6763 and by Estonian Information Technology Foundation.

REFERENCES

[1] M. Shahinpoor, "Ionic polymer-conductor composites as biomimetic sensors, robotic actuators and artificial muscles – a review", Electrochimica Acta 48 (2003), pp. 2343-2353.

[2] C. S. Kothera, "Characterization, Modeling, and Control of the Nonlinear Actuation Response of Ionic Polymer Transducers", Ph.D. dissertation, Dept. of Mechanical Engineering, Virginia Tech, 2005.

[3] K Mallavarapu, D. Leo, "Feedback Control of the bending response of ionic polymer actuators," Journal of Intelligent Material Systems and Structures, vol. 12, no. 3, pp. 143–155, 2001.

[4] R. Kanno, S. Tadokoro, M. Hattori, T. Takamori, K. Oguro, „Modeling of ICPF Actuator, Modeling of Electrical Characteristics" Proc. In IEEE 21st Intl Conf. On Industrial Electronics, Control, and Instrumentation, Vol. 2, pp. 913-918, 1995.

[5] R. Kanno, S. Tadokoro, T. Takamori, M. Hattori, K. Oguro, "Linear approximate dynamic model of an ICPF actuator", Proc. IEEE Intern. Conf. on Robotics and Automation, Vol. 1, pp. 219-225, Minneapolis, Apr. 1996.

[6] K. Newbury, D. Leo, „Linear Electro-mechanical Model of Ionic Polymer Transducers – Part I: Model Development", Journal of Intelligent Material Systems and Structures, vol. 14, no. 6, pp. 333–342, 2003.

[7] X. Bao, Y. Bar-Cohen, S. Lih, "Measurements and Macro Models of Ionomeric Polymer-Metal Composites (IPMC)," EAPAD Conference 2002, Proc. SPIE 4695, pp. 286-293, 2002.

[8] W. Yim, M. B. Trabia, J. M. Renno, "Dynamic Modeling of Segmented Ionic Polymer Metal Composite (IPMC) Actuator," Proc. IEEE/RSJ Int. Conf. on Intelligent Robots and Systems, 2006.

[9] K. Jung, J. Nam, and H. Choi, "Investigations on actuation characteristics of IPMC artificial muscle actuator," Sensors and Actuators A: Physical, Vol. 107, No. 2, 2003, pp. 183–192.

[10] R. C. Richardson, M. C. Levesley, M. D. Brown, J. A. Hawkes, K. Watterson, P. G. Walker, "Control of ionic polymer metal composites," IEEE/ASME Transactions on Mecatronics, Vol. 8, No. 2, 2003, pp.245–253.

[11] E. Weber, "Linear Transient Analysis", volume II., John Wiley and Sons, 1956.

[12] V. B. Rao, Delay analysis of the distributed RC line, Proceedings of the 32nd ACM/IEEE conference on Design automation, p.370-375, June 12-16, 1995.

[13] V. Szekely, "Distributed RC Networks," in " The circuits and filters handbook. 2nd ed." Wai Kai Chen (ed) 2003.

[14] B. Akle, D. Leo, "Correlation of capacitance and actuationin ionomeric polymer transducers," Journal of Materials Science 40 (2005) pp. 3715 – 3724.

[15] M. Shahinpoor and K. J. Kim, "Ionic polymer–metal composites: II. Manufacturing techniques," Smart Mater. Struct. 12, 2003, pp. 65–79.